

**Cotransport of human adenoviruses with clay colloids and TiO<sub>2</sub> nanoparticles in saturated porous media: Effect of flow velocity**

by

Vasiliki I. Syngouna<sup>1,\*</sup>, Constantinos V. Chrysikopoulos<sup>1</sup>, Petros Kokkinos<sup>2</sup>,  
Maria A. Tselepi<sup>2</sup>, and Apostolos Vantarakis<sup>2</sup>

<sup>1</sup>*School of Environmental Engineering, Technical University of Crete, 73100 Chania, Greece*

<sup>2</sup>*Environmental Microbiology Unit, Department of Public Health, University of Patras, 26500 Patras, Greece*

**Supporting data**

**Key words:** Human adenoviruses, clay minerals, KGa-1b, STx-1b, TiO<sub>2</sub> nanoparticles, cotransport.

April 10, 2017

\*Corresponding author (tel.:+ 306974665994, email: vsyngouna@isc.tuc.gr)

## 1. Calibration curves

Calibration curves were used to predict the concentration of KGa-1b, STx-1b and TiO<sub>2</sub> NP samples. The standards were run in sterile DNase I reaction buffer, as were the particle samples in column experiments. A few concentrations above and below the expected particle concentrations were measured. Clearly, Fig. S1 shows that all three calibration curves were of the linear form:  $y=mx+b$ , where  $m$  is the slope and  $b$  is the y-intercept.

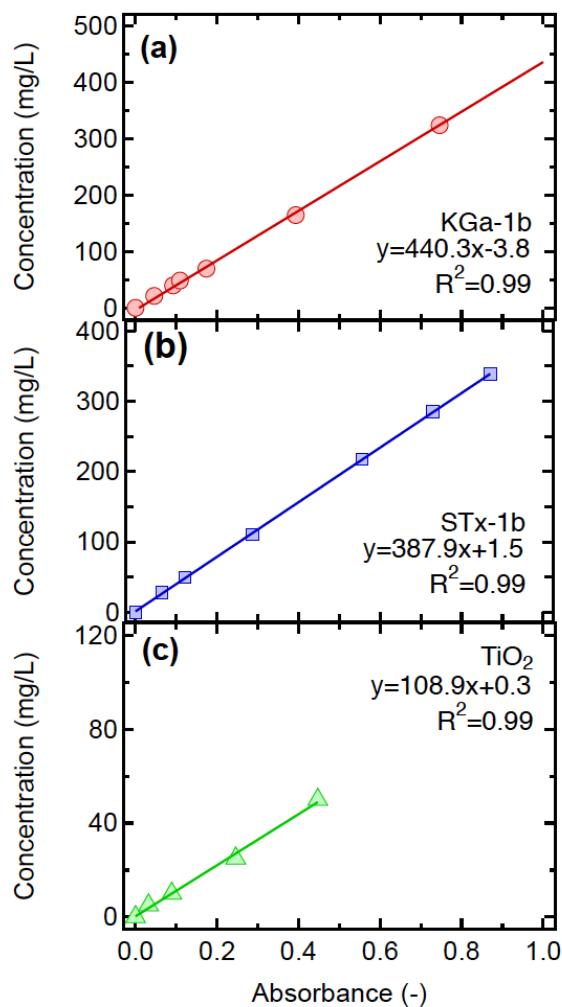


**Fig. S1.** Calibration curves for: (a) KGa-1b, (b) STx-1b, and (c) TiO<sub>2</sub> NPs

## 2. Morphology of TiO<sub>2</sub> NPs data

Transmission electron microscopy (TEM) by a JEOL (JEM-2100 system, operated at 200 kV) was performed by diluting NPs suspension in ddH<sub>2</sub>O, placed in an ultrasonic bath for 10 min, and air-dried onto a carbon-coated copper grid (200 mesh). A representative image is shown in Fig. S2. The TEM analyses suggested that TiO<sub>2</sub> nanoparticles in ddH<sub>2</sub>O created aggregates with size ~300 nm.

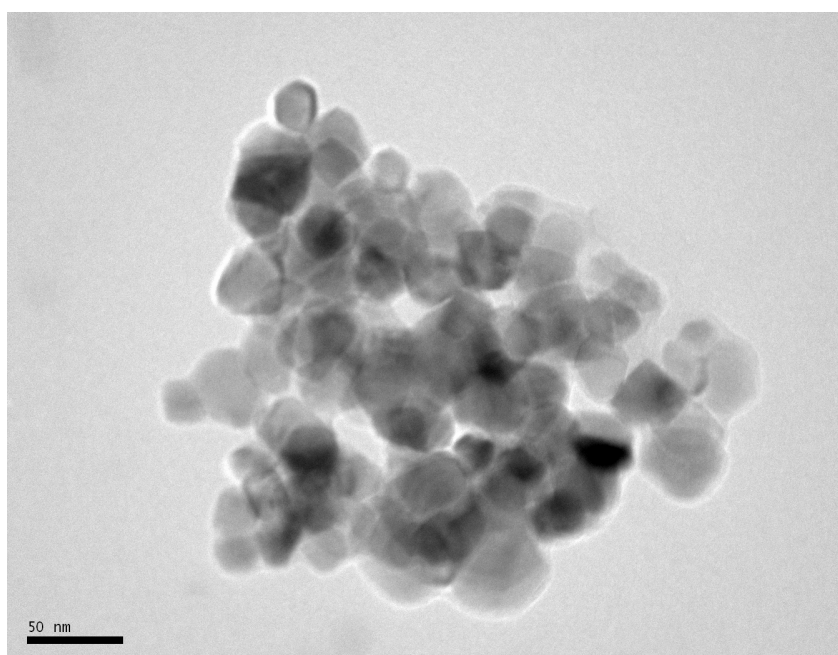


**Fig.S2.**Transmission electron micrographs of TiO<sub>2</sub> (anatase) in ddH<sub>2</sub>O

## 3. DNase-I protection assay

A volume of 2.5  $\mu$ L DNase I (RNase-free, 2000 units/mL, New England BioLabs Inc.) was added to 137.5  $\mu$ L of each sample and then all aliquots were incubated at 37°C for two hours. DNase-I is expected to degrade any viral DNA that is no longer protected by the viral capsid. Following the enzymatic digestion step, all samples were immediately processed for nucleic acids extraction. In detail, 140  $\mu$ L of each sample was added (separately) to 560  $\mu$ L of Lysis Buffer AVL, with 5.6  $\mu$ L of carrier RNA (QIAamp viral RNA mini kit, Qiagen). The DNase-I enzyme is inactivated

after the addition of the lysis buffer. The viral DNA was extracted according to the kit manufacturer's instructions, and the final volume was 100  $\mu$ L. The extracts were immediately stored at  $-80^{\circ}\text{C}$ .

#### 4. Colloid filtration theory data

The collision efficiencies,  $\alpha_{\text{Total-v}}$ , for human adenoviruses and  $\alpha_p$ , for clay colloids and  $\text{TiO}_2$  NPs were calculated for the transport and cotransport experimental conditions of this study using Eq. (4), where the single collector removal efficiency,  $\eta_0$  values were estimated from an existing correlation equation (Tufenkji and Elimelech, 2004), using the following parameter values (Table S1).

**Table S1.** Measured and calculated CFT parameter values

Parameter (Units of measurement)		Adenovirus (HAdV35)	Kaolinite (KGa-1b)	Montmorillonite (STx-1b)	$\text{TiO}_2$ NPs
$r_p$	Particle radius (m)	3.50E-08	4.21E-07	5.94E-07	9.00E-08
$r_c$	Collector radius (m)	2.00E-03	2.00E-03	2.00E-03	2.00E-03
$\rho_p$	Particle density ( $\text{kg/m}^3$ )	1340	2200	2200	3900
T	Absolute Temperature (K)	298	298	298	298
D	Diffusion coefficient ( $\text{m}^2/\text{s}$ )	7.00E-12	5.82E-13	4.13E-13	2.72E-12
$\rho_f$	Water density ( $\text{kg/m}^3$ )	999.7	999.7	999.7	999.7
$\mu$	Water viscosity ( $\text{Ns/m}^2$ )	8.91E-04	8.91E-04	8.91E-04	8.91E-04
$\theta$	Porosity (-)	0.42	0.42	0.42	0.42
As	Porosity - parameter (-)	33.64	33.64	33.64	33.64
$N_R$	Relative size number (-)	3.50E-05	4.22E-04	5.94E-04	9.05E-05
$N_{\text{vdw}}$	van der Waals number (-)	1.82E+00	1.82E+00	1.82E+00	1.82E+00
Parameter (Units of measurement)		<b>Q=2.5 mL/min</b>			
U	Approach velocity (m/s)	8.50E-05	8.50E-05	8.50E-05	8.50E-05
$N_A$	Attraction number (-)	2.14E+00	1.48E-02	7.46E-03	3.21E-01
$N_{\text{Pe}}$	Peclet number (-)	2.43E+04	2.93E+05	4.12E+05	6.28E+04
$N_G$	Gravity number (-)	1.20E-05	6.14E-03	1.22E-02	6.84E-04
Parameter (Units of measurement)		<b>Q=1.5 mL/min</b>			
U	Approach velocity (m/s)	5.20E-05	5.20E-05	5.20E-05	5.20E-05
$N_A$	Attraction number (-)	3.53E+00	2.43E-02	1.23E-02	5.28E-01
$N_{\text{Pe}}$	Peclet number (-)	1.48E+04	1.78E+05	2.50E+05	3.82E+04
$N_G$	Gravity number (-)	1.97E-05	1.01E-02	2.00E-02	1.12E-03
Parameter (Units of measurement)		<b>Q=0.8 mL/min</b>			
U	Approach velocity (m/s)	2.70E-05	2.70E-05	2.70E-05	2.70E-05

$N_A$	Attraction number (-)	6.75E+00	4.71E-02	2.38E-02	1.02E+00
$N_{Pe}$	Peclet number (-)	7.72E+03	9.18E+04	1.29E+05	1.97E+04
$N_G$	Gravity number (-)	3.78E-05	1.96E-02	3.88E-02	2.18E-03

## 5. Electrokinetic Measurements

The zeta potentials were measured by the zetasizer (Nano ZS90, Malvern Instruments, Southborough, MA), following the procedure outlined by Syngouna and Chrysikopoulos (2010). The zeta potential of the hAdV35s, measured at pH 7.6 in sterile DNase I reaction buffer ( $I_S=1.4 \times 10^{-3}$  M) was found to be equal to  $-21.78 \pm 1.39$  mV (Kokkinos et al., 2015). The Zeta potentials of the clays colloids, measured at pH 7 in sterile ddH<sub>2</sub>O ( $I_S=10^{-4}$  M), were found to be equal to  $-26.03 \pm 2.77$  mV for KGa-1b, and  $-20.5 \pm 0.8$  mV for STx-1b (Syngouna and Chrysikopoulos, 2013). The zeta potential of the TiO<sub>2</sub> (anatase) NPs used in this study was measured at pH 7 in sterile ddH<sub>2</sub>O ( $I_S=10^{-4}$  M) and was determined to be  $-23.67 \pm 0.88$  mV (Syngouna and Chrysikopoulos, 2017). Furthermore, the zeta potential of glass beads stored in ddH<sub>2</sub>O at pH 7 was found to be equal to  $-54.6 \pm 2.4$  mV (Syngouna and Chrysikopoulos, 2013). All zeta potential measurements were obtained in triplicates.

For soft particles as human adenoviruses, the electrical double layer is formed not only outside but also inside the surface charge layer, consequently the zeta potential becomes less important and for some cases, loses its physical meaning (Duval and Gaboriaud, 2010). In this study, the electrokinetic zeta potentials were used instead of the surface potentials. Note that the conventional DLVO interaction models were used, assuming that hAdV35 particles behave as hard spheres.

## 6. DLVO interaction energy calculations

Virus, clay colloid and TiO<sub>2</sub> NPs retention by the packed column and adsorption onto glass beads greatly depends on the total DLVO interaction energy. To better understand the observed virus- glass beads, clays-glass beads and TiO<sub>2</sub>-glass beads interactions in the column experiments

conducted in this study, the total interaction energy was calculated following the procedure described in Chrysikopoulos and Syngouna (2012) for the sphere-plate geometry approximation (see Fig. S3, Table S2). Note that the total interaction energy  $\Phi_{DLVO}$  [J] equals the sum of the van der Waals,  $\Phi_{vdW}$  [J], the electrostatic double layer,  $\Phi_{dl}$  [J] and the Born,  $\Phi_{Born}$  [J] interaction energies over the separation distance  $h$  [L] between the approaching surfaces (Loveland et al., 1996). Moreover, in order to evaluate the possibility of particle aggregation, the  $\Phi_{DLVO}$  interaction energy profiles for the case of sphere-sphere approximation as applied to identical virus-virus and particle-particle interactions were constructed under the experimental conditions (see Fig. S4, Table S3).

**Table S2.** Calculated critical points ( $\Phi_{min1}$ ,  $\Phi_{max1}$ ,  $\Phi_{min2}$ ) of the DLVO interaction energy profiles for virus-glass beads, clays-glass beads, and  $TiO_2$ -glass beads.

Sphere- plate model	$\Phi_{min1}$ ( $k_B T$ )	$\Phi_{max1}$ ( $k_B T$ )	$\Phi_{min2}$ ( $k_B T$ )
HAdV35	-24.44	30.63	-0.0071
KGa-1b	na	513.4	-0.0826
STx-1b	-547.9	465.4	-0.1223
$TiO_2$	-58.2	90.61	-0.0257

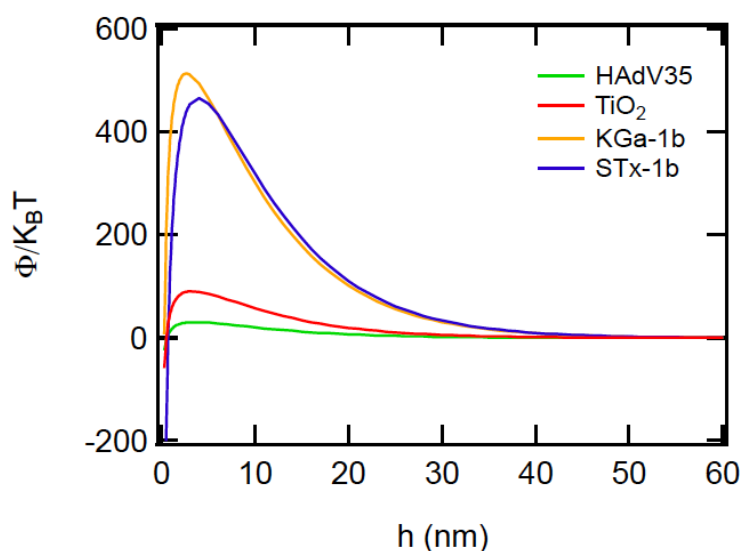


**Fig. S3.** Predicted sphere-plate  $\Phi_{DLVO}$  interaction energy profiles for: HAdV35 and glass beads, TiO<sub>2</sub> NPs and glass beads, KGa-1b and glass beads, and STx-1b and glass beads, as a function of separation distance (here pH=7.6,  $I_S=1.4 \times 10^{-3} M$ ).

**Table S3.** Calculated critical points ( $\Phi_{min1}$ ,  $\Phi_{max1}$ ,  $\Phi_{min2}$ ) of the DLVO interaction energy profiles for HAdV35-hAdV35, (KGa-1b)-(KGa-1b), (STx-1b)-(STx-1b), (TiO<sub>2</sub>)-(TiO<sub>2</sub>).

Sphere-sphere model	$\Phi_{min1}$ (k <sub>B</sub> T)	$\Phi_{max1}$ (k <sub>B</sub> T)	$\Phi_{min2}$ (k <sub>B</sub> T)
HAdV35-hAdV35	na	na	-1.001
(KGa-1b)-(KGa-1b)	na	na	-9.084
(STx-1b)-(STx-1b)	na	na	-11.79
(TiO <sub>2</sub> )-(TiO <sub>2</sub> )	na	na	-2.954

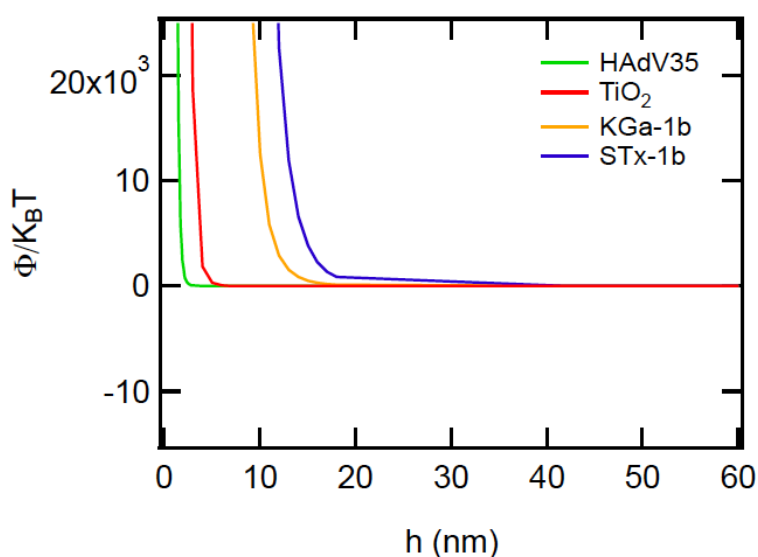


**Fig. S4.** Predicted sphere-sphere  $\Phi_{DLVO}$  interaction energy profiles for: HAdV35-hAdV35, (TiO<sub>2</sub>)-(TiO<sub>2</sub>), (KGa-1b)-(KGa-1b), and (STx-1b)-(STx-1b) interactions, as a function of separation distance (here pH=7.6,  $I_S=1.4 \times 10^{-3} M$ ).

## References

- Chrysikopoulos, C.V., Syngouna, V.I., 2012. Attachment of bacteriophages MS2 and  $\Phi$ X174 onto kaolinite and montmorillonite: extended DLVO interactions. *Colloids Surf. B: Biointerfaces* 92, 74-83.
- Duval, J.F.L., Gaboriaud, F., 2010. Progress in electrohydrodynamics of soft microbial particle interphases. *Current Opinion in Colloid & Interface Science* 15, 184–195.
- Kokkinos, P., Syngouna, V. I., Tselepi, M. A., Bellou, M., Chrysikopoulos C. V., Vantarakis A., 2015. Transport of human adenoviruses in water saturated laboratory columns. *Food and Environmental Virology* 7 (2), 122-131.
- Loveland, J.P., Ryan, J.N., Amy, G.L., Harvey, R.W., 1996. The reversibility of virus attachment to mineral surfaces. *Colloids Surf. A: Physicochem. Eng. Aspects* 107, 205-221.
- Syngouna, V I., Chrysikopoulos, C.V., 2015. Experimental investigation of virus and clay particles cotransport in partially saturated columns packed with glass beads. *Journal of Colloid and Interface Science* 440, 140-150.
- Syngouna, V I., Chrysikopoulos, C.V., 2017. Inactivation of MS2 bacteriophage by titanium dioxide nanoparticles in the presence of quartz sand with and without ambient light. *Journal of Colloid and Interface Science*, 497, 117–125.
- Syngouna, V. I., Chrysikopoulos, C. V., 2013. Cotransport of clay colloids and viruses in water saturated porous media. *Colloids and Surfaces A* 416, 56–65.
- Syngouna, V.I., Chrysikopoulos, C. V., 2010. Interaction Between Viruses and Clays in Static and Dynamic Batch Systems. *Environmental Science and Technology* 44 4539–4544.
- Tufenkji, N., Elimelech, M., 2004. Correlation equation for predicting single-collector efficiency in physicochemical filtration in saturated porous media. *Environmental science and technology* 38 (2), 529-5